FUNCTIONAL AND ONTOGENETIC IMPLICATIONS OF BITE STRESS IN ARTHRODIRE PLACODERMS

ERIC SNIVELY
Mechanical Engineering, Russ College of Engineering and Technology
Ohio University, Athens, Ohio 45701
es180210@ohio.edu

PHILIP S. L. ANDERSON
Department of Earth Sciences, University of Bristol, Wills Memorial Building
Queen's Road, Bristol BS8 1RJ, United Kingdom

AND **MICHAEL J. RYAN**
Department of Vertebrate Paleontology
Cleveland Museum of Natural History, 1 Wade Oval Drive, Cleveland, Ohio 44106

ABSTRACT

Arthrodires were predatory vertebrates of the Devonian seas, with simple lower jaws conducible to examination of feeding across growth, evolution, and local diversity. 2D finite element analyses (FEA) of arthrodire mandibles (scaled to equivalent length and force, and checked against a 3D control), and a new method of stress integration, enable extensive comparisons of bite stress. FEA indicates that juveniles of Cleveland Member *Dunkleosteus terrelli* had robust mandibles, and could shear into tough prey tissues similarly to adults. Low mandible rotational inertias of some Gogo Formation arthrodires suggest rapid jaw depression for suction feeding, whereas others had low mandible stress suggesting greater bite force. These results point to high trophic diversity of Gogo arthrodires in their reef habitats, and high predatory competence of young *Dunkleosteus*.

Introduction

Arthrodire placoderms were successful Late Devonian predators, as open marine forms recorded in the North American Cleveland Member of the Ohio Shale (Figure 1A–C) and as reef dwellers (Figure 1E–J) preserved in the Gogo Formation of Australia (Playford, 1980; Jaminski et al., 1998; Long and Trinajstik, 2010). The diversity of arthrodires and the simplicity of their lower jaws (consisting of a posterior blade and anterior dental regions: Anderson, 2008) have elicited productive characterizations of feeding in these basal gnathostomes (Carr, 1995; Anderson, 2008, 2009; Anderson and Westneat, 2007, 2009). Anderson (2008, 2009) applied geometric morphometrics, moment arm analysis, and jaw second moments of area to explore morphological and functional variation in feeding arthrodires. Anderson and Westneat (2007, 2009) examined more dynamic functions with musculoskeletal kinematic modeling of jaws in *Dunkleosteus terrelli*. Further studies have extended the kinematic modeling to other arthrodires (Anderson, 2010).

We introduce two additional methods to elicit hypotheses and to evaluate the functional performance of arthrodire jaws. Finite element (FE) analysis is common for estimating stresses and strains in skull elements (Ross, 2005; Rayfield, 2007, and references in each). Across surfaces or within modeled bones, histograms of stress at sampled points (nodes in an FE model) are valuable for comparing structural performance in different taxa (Slater et al., 2009; Tseng, 2009; Tseng and Binder, 2009). We use curve fitting and simple differential equations to graph and compare stresses across hundreds of points. This method facilitates higher-resolution evaluation of stresses than histograms of only a few points and simplifies comparisons of stress magnitude in given regions of a mandible.

Rotational inertias (*RI*) of their mandibles influenced how quickly arthrodires could open their jaws and are a reasonable inverse indicator of suction-feeding performance. Suction feeding in gnathostomes is effective with rapid expansion of the oral cavity, hypothesized for large arthrodires by Anderson and Westneat (2009). For a given abductive (jaw opening) torque τ_j, a lower rotational inertia of the lower jaw will increase its angular acceleration α_j, rate of opening, and effectiveness of suction feeding. Although low *RI* of inferognathals does not confirm suction feeding to the exclusion of other mechanisms, *RI* is one measure of biomechanical performance for deriving such hypotheses of feeding style.

Phylogenetic, functional, and morphological aspects of arthrodire feeding style are more thoroughly explored elsewhere (Anderson, 2008, 2009, 2010; Anderson and Westneat, 2007). We focus here on the utility of our methods for exploring such
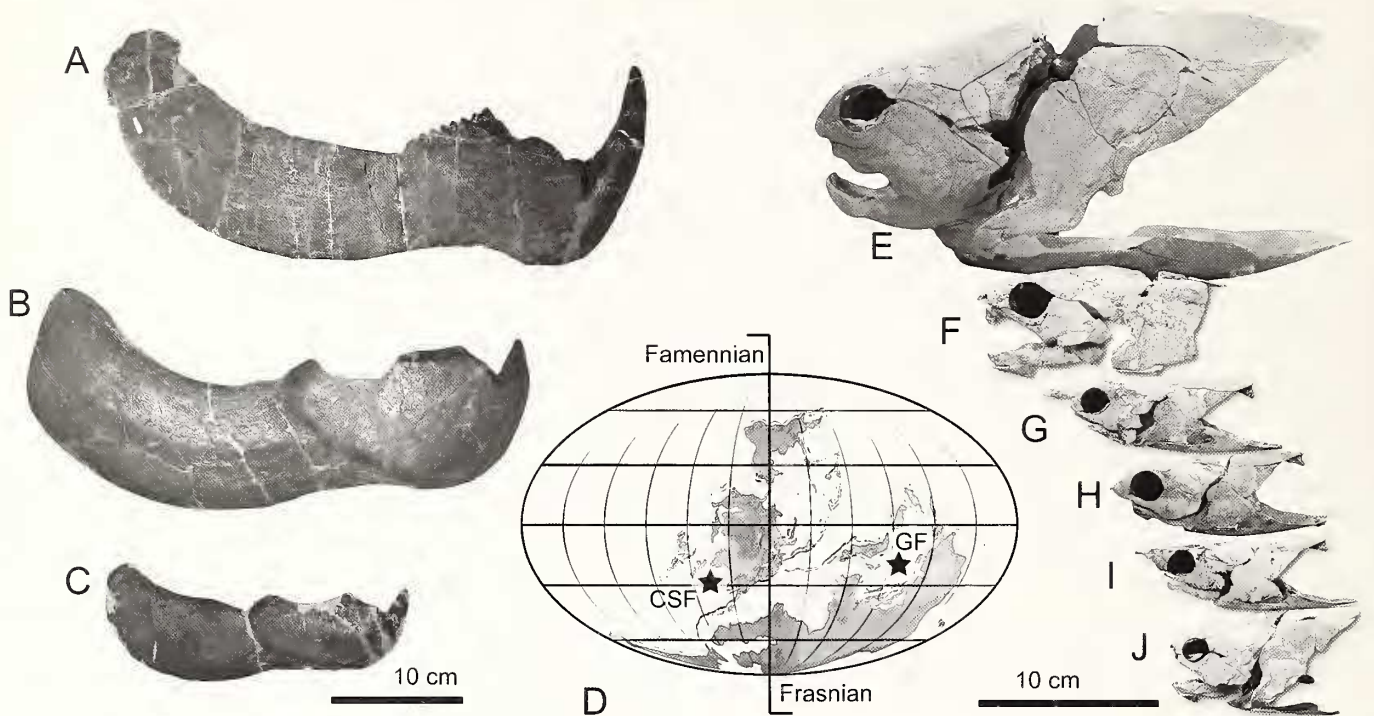
Figure 1. Arthrodire specimens analyzed for this study. Inferognathals of A, *Gorgonichthys clarki* (CMNH) and B, C, adult and juvenile *Dunkleosteus terrelli* (CMNH) from the Cleveland Member (CSF = Cleveland Shale Formation, superseded). D, Paleomap of the late Devonian (after Blakey, 2010) showing locations of Cleveland Member and Gogo Formation habitats. E, *Eastmanosteus calliaspis*. F, *Incisoscutum sarahae*. G, *Fallacosteus turnarae*. H, *Latocamuris coulthardi*. I, *Camuropiscis concinnus*. J, *Mcnamaraspis kaprios*. Note similar mandible shapes in *Dunkleosteus*, *Gorgonichthys*, and *Eastmanosteus*, and the relative slenderness of the blade and large size of the anterior cusp in *Gorgonichthys* compared with those of *Dunkleosteus*.

questions and to test three hypotheses of feeding ontogeny and function. Some large *Dunkleosteus terrelli* inferognathals appear more gracile than smaller ones, yet more robust than the inferognathals of their large contemporary, *Gorgonichthys clarki*. The deep lower jaw in small *Dunkleosteus* specimens suggests that such individuals had lower inferognathal stresses than large adult *Dunkleosteus* per unit bite force and jaw length (hypothesis 1). Mandibles of *Gorgonichthys* are predicted to have the highest relative stress.

Mandibles of Gogo Formation arthrodires vary more than those of large predaceous forms from the Cleveland Member. The basal pachyosteomorph *Eastmanosteus* (Carr, 1991; Anderson, 2009) has a long, tall dental region, and Anderson (2009) quantitatively identified it as a potential generalist feeder. At the other pole of mandible shape is the mandible of the coccosteomorph *Camuropiscis*, which has a slender anterior portion and a deep posterior blade. These shape differences and second moments of area of the jaws (Anderson, 2009) suggest two hypotheses. One hypothesis is that *Eastmanosteus* had lower stress in the anterior portion of the mandible per unit jaw length than in other Gogo taxa (hypothesis 2), indicating greater bite force. The other hypothesis is that the slender anterior portion of the mandible in *Camuropiscis* indicates that it had lower rotational inertia than in the other examined Gogo arthrodire mandibles (hypothesis 3), contributing to rapid expansion of the jaws and potentially effective suction feeding on small prey.

In this paper the abbreviation CMNH designates the Cleveland Museum of Natural History.

Materials and Methods
Finite element models

We constructed sagittal representations of the inferognathals after the methods of Rayfield (2004), Shychoski (2006), and Snively and Cox (2008). Point-by-point tracings of the jaws in lateral view (scaled to their original size) were saved as DXF coordinates and imported into Comsol Multiphysics for meshing and application of material properties. For comparability we scaled the models to the same length of 300 mm. (Scaling them to same surface area [Dumont et al., 2009] is better for performance comparisons, but would have given forms with a tall dental region a greater advantage, and tested hypotheses 1 and 2 less stringently.) FE meshes consisted of approximately 20,000 triangle elements for each model. Because material properties of semidentine are unknown, we assigned uniform properties to the dental region and blade of each inferognathal (density = 1850 kg/m^3, elastic modulus = 20 GPa, Poisson's ratio = 0.3). These are realistic properties for dentine and dense compact bone without extensive Haversian reworking (a common histology for placoderm lower jaws: Mark Wilson, personal communication, 2010).

Forces and constraints

For FE comparisons of the Gogo Formation and Cleveland Member arthrodires and respective comparisons within these faunas, we applied equivalent forces and constraints to all 300-mm models. These were 300 N of adductor muscle force and 100 N force at the anterior cusp or equivalent position in
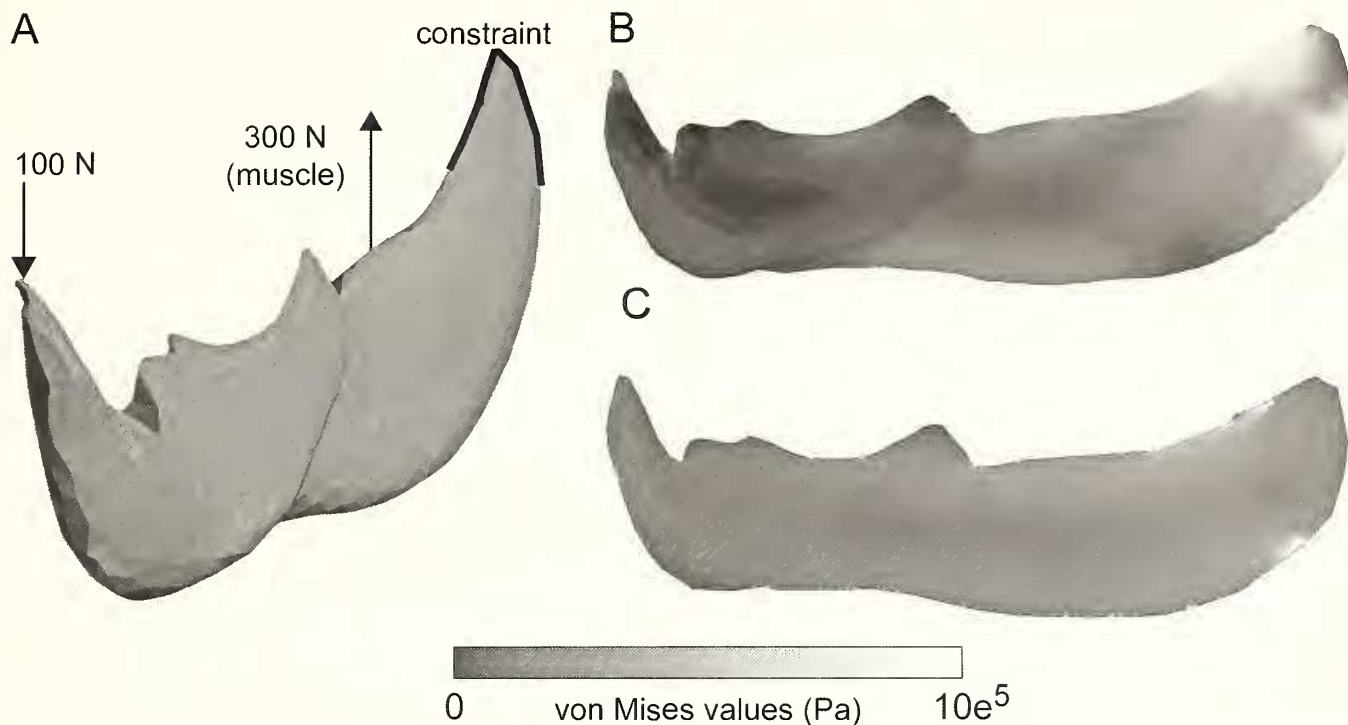
Figure 2. 2- and 3D finite element inferognathal models of *Dunkleosteus terrelli* experience similar von Mises stresses, supporting the use of 2D vs. 3D models for comparisons of the blade region. Bite force (100 N) is applied to the anterior cusp, and muscle force (300 N) to the middle of the blade. A, 3D model in oblique view. B, 3D model in lateral view. C, 2D projection model. Higher stresses occur in the 3D model at the point of force application, but stress magnitudes and distribution are nearly identical in the blade regions.

specimens that lack this structure (Figure 2A). To allow the jaws to deform and to prevent free rotation, all models were constrained at the jaw joint along the posterior periphery of the lower jaw. We did not constrain the specimens at the bite point to ensure that the structures could deform at this position.

3D-control FEA for 2D models

We assessed the realism of sagittal 2D models against a 3D model of a *Dunkleosteus* inferognathal (Figure 2). Several specimens were CT scanned at Canada Diagnostics Centre (Calgary, Alberta). Scan data of one inferognathal (CMNH 7069) was converted to an FE model with 40,000 elements with Mimics (Materialise), using methods of Wroe et al. (2007), Arbour and Snively (2009), and Bell et al. (2009). Equivalent forces, properties, and constraints were then applied to 2- and 3D representations.

Stress comparisons

Von Mises stress (a sum of stress principal components at nodes) was used for visualizing stress distribution and assessing structural performance of the jaws. Von Mises is a good index of relative proximity to yield stress, and its distribution parallels that of strain energy density (Bell et al., 2009). Because it does not yield strict values for compression and tension, von Mises facilitates fine-scaled, visual comparisons of regional stress using a grayscale color palette.

We compared von Mises stress quantitatively by determining equations of best fit for stresses along regions of jaws and by plotting and integrating the equations; areas under the curves gave indices of total stress. We drew transects in Multiphysics where relatively high stress occurred in the jaws: the dental region for

Gogo arthrodires and the dorsal region of the blade in *Dunkleosteus* and *Gorgonichthys*. Results for 200 points along the transects were exported into Microsoft Excel as readings of radial position versus stress. We used Excel to calculate lines of best-fit, high-degree exponential functions that are only meaningful within the positional bounds of the transects. These became functions F of differential equations of the change of stress (S) versus position (p).

$$F(S) = \frac{dS}{dp}$$

Total stress was evaluated by solving the definite integral for $F(S)$ from the starting position ($p = 1$) to the endpoint of the transect ($p = n$; in this case $n = 200$).

$$\sum S = \int_{1}^{n} c_{(x)} p^x \ldots + c_{(x=1)} p^0$$

Here "c" represents coefficients, and "x" the degrees of the terms for each position. This method complements the common graphical representation of stress versus position, by giving comparative values for total stress while sampling stress at many more positions.

Relative rotational inertias

Our methods for calculating relative *RI* were similar to those of Henderson and Snively (2003), but with simplified segment masses. We scaled inferognathals of *Camuropiscis*, *Eastmanosteus*, *Fallacosteus*, *Latocamurus*, *Incisoscutum*, and *Mcnamaraspis* to
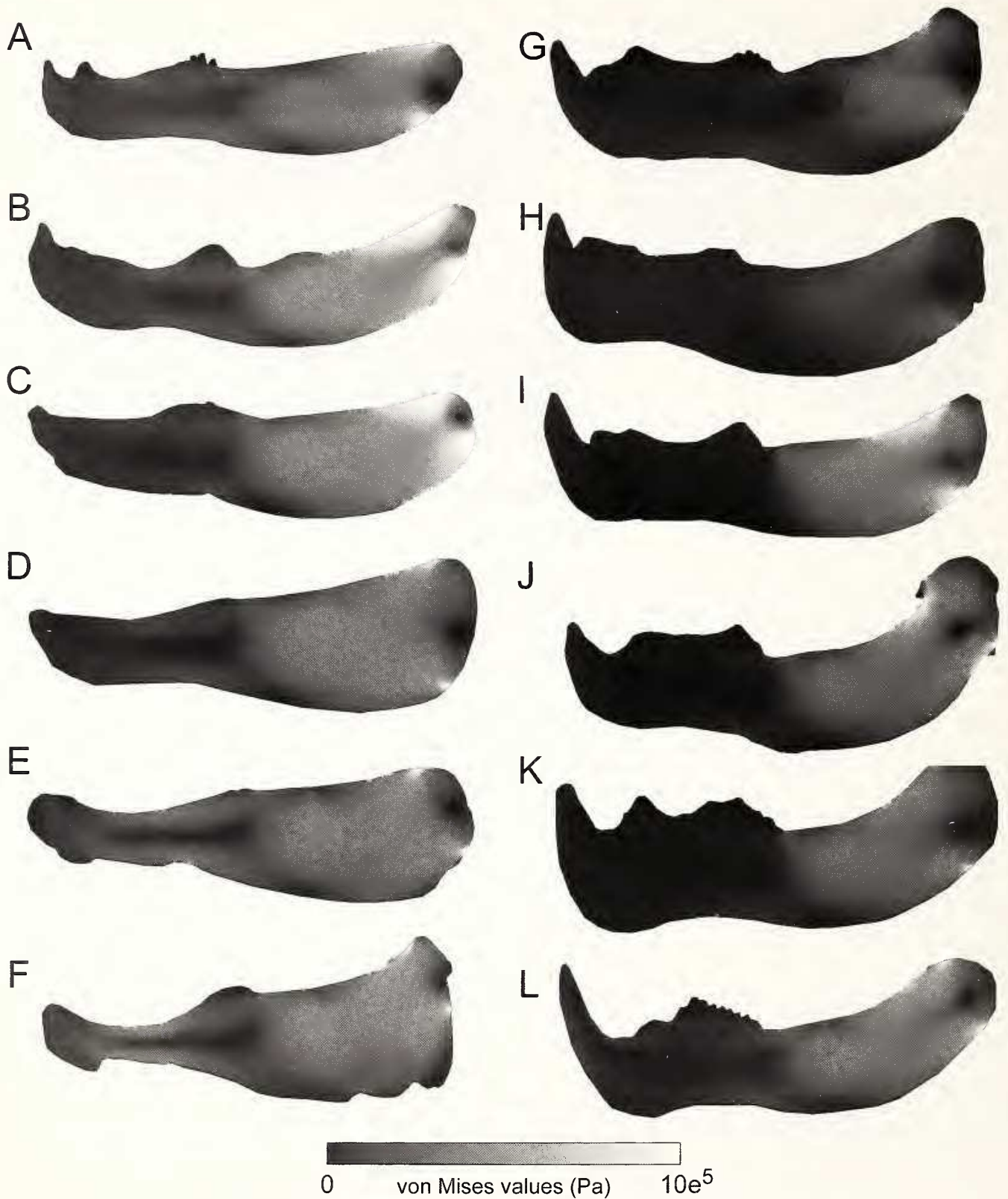
Figure 3. Stress magnitudes and distributions in examined arthrodire inferognathals, with all specimens scaled to 30 cm. Increasing von Mises stresses are color coded from dark (lowest) to white (highest). A–F are Gogo Formation specimens. A, *Mcnamaraspis kaprios*. B, *Eastmanosteus calliaspis*. C, *Incisoscutum sarahae*. D, *Latocamurus coulthardi*. E, *Fallacosteus turnarae*. F, *Camuropiscis concinnus*. G–J, *Dunkleosteus terrelli*, from smallest (20 cm) to largest (55 cm) original lengths. K, *Dunkleosteus terrelli* specimen with posterior blade restored; estimated length 65 cm. L, *Gorgonichthys clarki*, approximately 42 cm. Stresses increase in the region anterior to the blade in A–F and in the dorsal part of the blade of Cleveland Member arthrodires; stresses are generally higher in originally larger specimens.
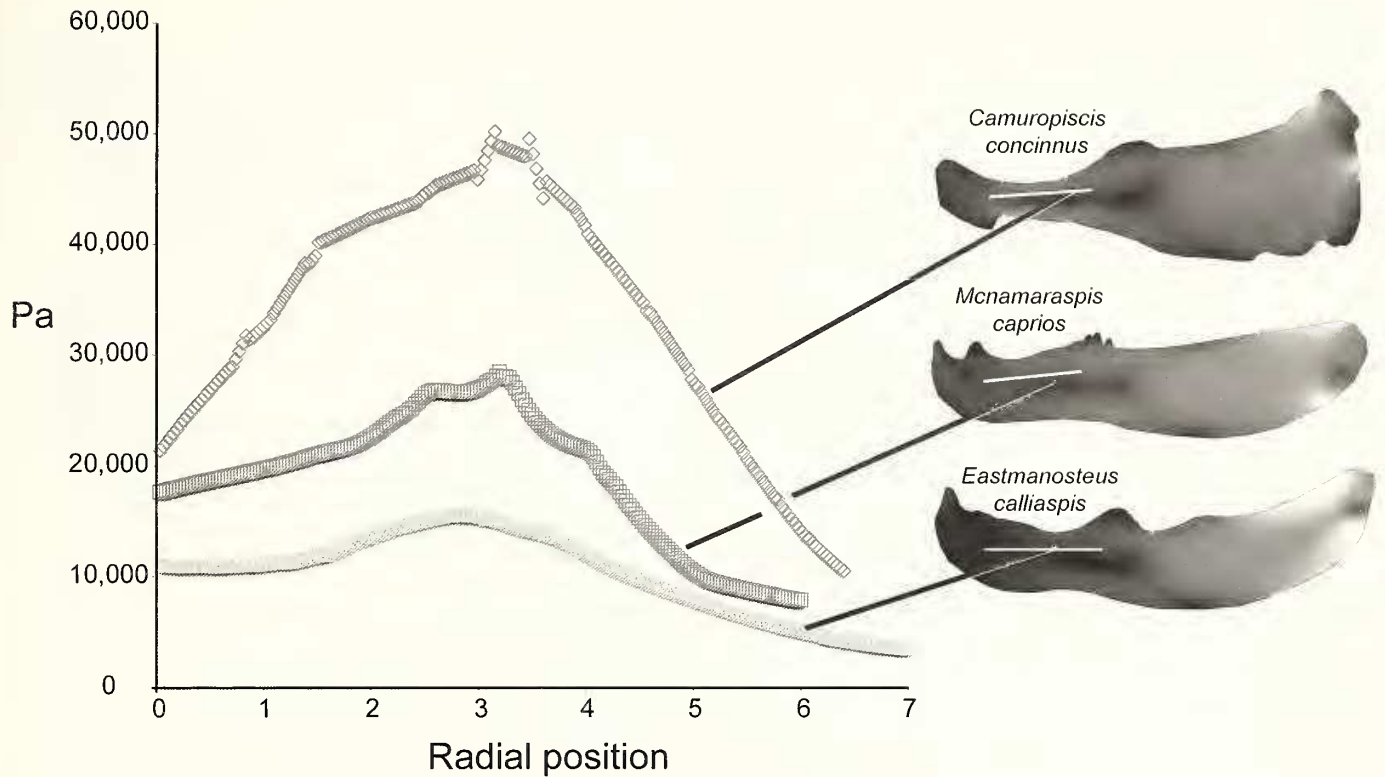
Figure 4. Integrated mandible stresses in three Gogo Formation arthrodires, graphing von Mises stresses in an anterior transect of each mandible (Pa) as a function of radial position within the transect. All specimens are scaled to 300 mm in length. The *Camuropiscis* mandible experienced much higher anterior stresses than the others.

3 cm in length with the same assumed thickness, and divided them anteroposteriorly into 17 segments. *RI*s were then calculated by adding segment *RI*s using the parallel axis theorem (Henderson and Snively, 2003)

$$RI = \sum m_i r_i^2$$

in which m_i is the mass of a segment, and r_i is its distance from the center of rotation (in this case the jaw joint). Because each segment has the same length and width, its height becomes a proxy for mass.

Results
Patterns of von Mises values
Comparing 2- and 3D models is informative about interpreting 2D results (2D models are not strictly validated, which in FEA requires checking results against physical displacements). 3D and 2D models of a *Dunkleosteus* inferognathal show similar stress distributions in the blade region and in the ventral portion of the dental region (Figure 2). However, higher stress occurs at the point of force application (the anterior-cusp tip) on the 3D model. This verifies that comparative interpretations of stress in the 2D models posterior to the dental region, and even in the ventral part of the dental region itself, gives the same basic pattern as the 3D models. The results suggest that stresses will be higher than indicated in the 2D models along pointed structures and cutting edges of the jaws, even though the 2D models represent "thin" sagittal slices.

Stress magnitudes vary substantially with shape and region in arthrodire mandibles scaled to the same lengths and forces (Figure 3). Stresses are biologically interpretable away from the highest values, which occur at transitions between constrained and unconstrained regions (Saint-Venant's principle: Cook, 1995). All inferognathals experience comparatively high yet diffuse stresses in the blades (post-dental regions), ventral to where muscle forces are applied. Muscle-induced stresses appear lower in blades of Cleveland Member forms than in Gogo Formation specimens, except in a large gracile *Dunkleosteus* (Figure 3G) and the *Gorgonichthys* specimen (Figure 3L). The dental portions behave like cantilevered beams, with central regions of lower stress approximating a neutral axis. Stresses are higher in the dental regions of the Gogo Formation arthrodires (Figure 3A–F) than in *Dunkleosteus* and *Gorgonichthys* specimens from the Cleveland Member (Figure 3G–L). Dental-region stresses increase from forms categorized functionally as "generalists" and "choppers" (e.g. *Mcnamaraspis* and *Dunkleosteus*) to "biters" (*Camuropiscis*; Anderson, 2008).

Integrated stress and relative rotational inertias
For anterior transects of Gogo specimens (Figure 4), integrated stress diminishes from 212,020 Pa for *Camuropiscis concinnus* to 114,569 Pa for *Mcnamaraspis caprios*, and to 66,682 Pa in *Eastmanosteus calliaspis*. The *Camuropiscis* mandible experienced twice the peak stress as in *Mcnamaraspis*, and four times that of *Eastmanosteus*. Von Mises values along the mandible blade in Cleveland Member arthrodires are higher than in the dental regions of the Gogo Formation forms. Integrated stresses for the
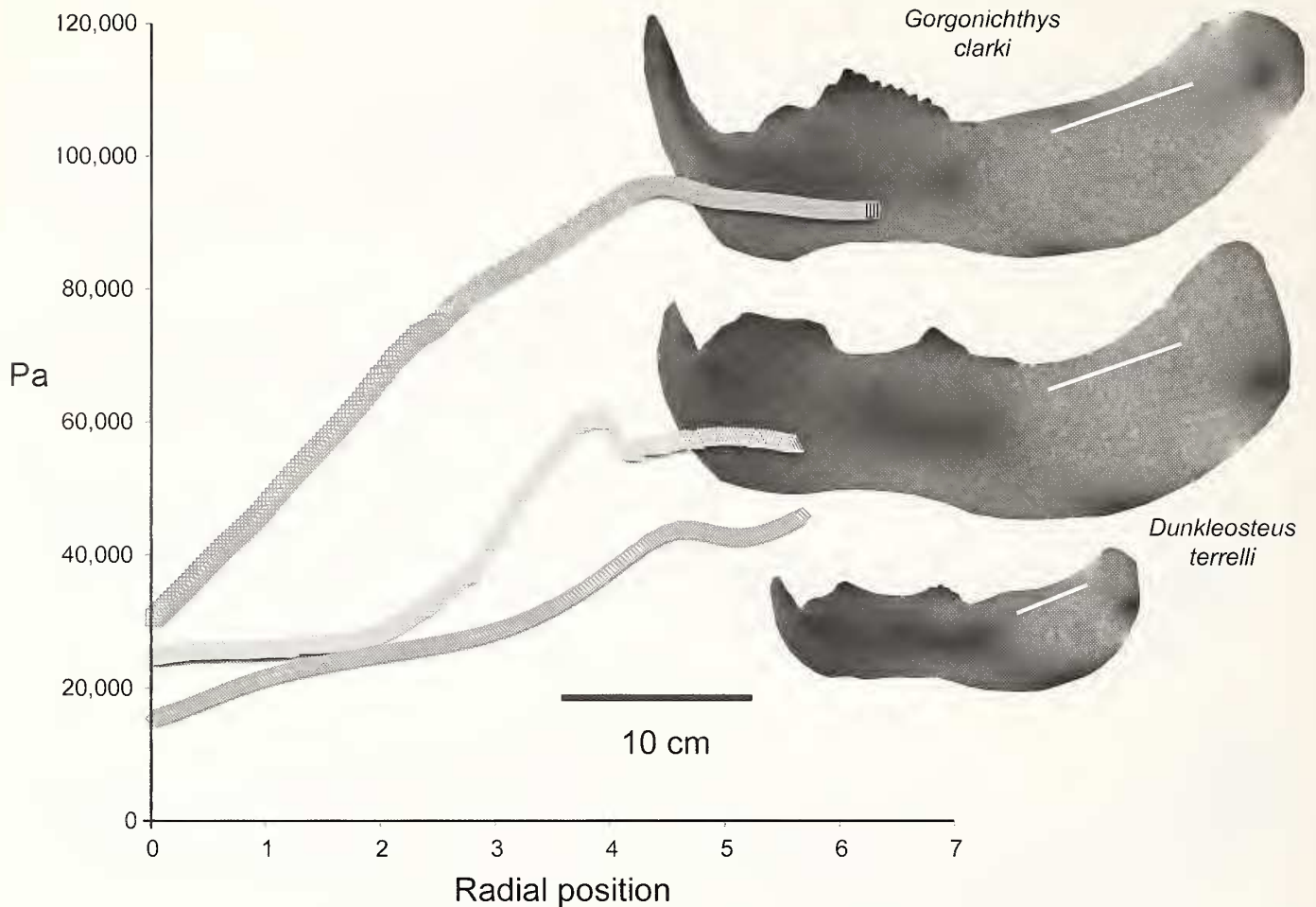
Figure 5. Integrated mandible stresses in Cleveland Member arthrodires, graphing von Mises stresses (Pa) in the dorsal portion of each blade as a function radial position. Specimens are scaled to 300 mm each. White lines across the specimens indicate transects of stress results.

Cleveland Member forms (Figure 5) are 444,841 Pa (445 kPa) in the large *Gorgonichthys clarki*, 260 kPa in the adult *Dunkleosteus terrelli*, and 118 kPa in the juvenile.

Relative rotational inertias for Gogo arthrodires are listed in Table 1. *Mcnamaraspis* and *Eastmanosteus* have the highest relative *RI*s (22–23), 16–20% higher than in *Camuropiscis*, which has the lowest *RI*. *Latocamuris* and *Fallacosteus* also have comparatively low *RI*s. Most of the specimens were of similar absolute size (Figure 1), and the relative *RI*s reflect absolute quantities. *Eastmanosteus* is much larger than the others, and the high relative *RI* of its mandible indicates a much higher inertia in life.

Table 1. Relative rotational inertias ($RI = \sum m_i r_i^2$) of representative Gogo arthrodires. "Mass" (m_i) is represented by the height of a given slice *i*, with equivalent thicknesses for all slices in all specimens.

Taxon	Relative *RI*
Camuropiscis	19.00
Eastmanosteus	22.06
Incisoscutum	20.09
Mcnamaraspis	22.81
Fallacosteus	19.60
Latocamuris	19.92

Discussion

Finite-element results for the Cleveland Member arthrodires suggest lower stresses in juvenile *Dunkleosteus* for a given jaw length (corroborating hypothesis 1), and relatively high stresses in *Gorgonichthys*. Lower relative stress in juvenile *Dunkleosteus* indicates the ability to accommodate high bite force, analogous to the adults which applied among the highest known bite forces (Anderson and Westneat, 2009). Indeed this pattern suggests slight negative allometry in *Dunkleosteus* bite force. The juveniles were likely able to shear into resistant prey tissues when biting, similarly to the adults but on a smaller scale, and to hunt a broader range of prey types than might be predicted from their smaller size. This contrasts with the condition common in tetrapods, including lizards and carnivorous dinosaurs (Rieppel, 1979; Currie, 2003; Therrien et al., 2005; Shychoski and Snively, 2008), in which the lower jaws of juveniles are more gracile than in adults. Using morphometrics (Anderson, 2008) and biomechanical studies of extant and fossil forms, we can test whether changes in *Dunkleosteus* bite force, through ontogeny and its available prey spectrum, are unusual among aquatic gnathostomes. In some cases the effects of both geometry and material properties can be assessed, as in white sharks whose jaws accrue additional layers of stiff calcified cartilage (Dingurkas et al., 1991), but may change overall shape isometrically as they grow.

Among the more diverse Gogo Formation arthrodires, finite element and rotational inertia results parallel Anderson's (2008, 2009) morphometric characterizations, yet complement possible feeding modes for *Fallacosteus* and *Camuropiscis*. As expected, *Mcnamaraspis* and *Eastmanosteus* (a generalist) have lower relative stress in and posterior to the dental region than *Camuropiscis* (a biter/grazer). High stress in this gracile region of *Camuropiscis* inferognathals suggests jaws well-suited to fine procurement and manipulation of prey, yet less suited to hard bites than in other arthrodires, despite flat anterior biting surfaces and a deep posterior mandible suggestive of durophagy.

Deep posterior and shallow anterior portions of the inferognathals in *Camuropiscis*, *Latocamuris*, and *Fallacosteus* imparted low sagittal rotational inertias about the jaw joint. This would have enabled rapid opening of the jaws, especially when coupled with high levels of kinematic transmission calculated for these groups from four-bar linkage models (Anderson, 2010). Rapid jaw abduction suggests effective suction feeding and rapid ingestion of prey. Biomechanical indicators of suction feeding do not falsify reef grazing or other means of procuring prey in *Camuropiscis* (including ingestion and crushing of crustaceans: Anderson, 2009). Instead, they offer an alternative hypothesis and/or complementary feeding mechanism open to further testing. In this and other cases, consideration of the role and function of articular cartilage will greatly aid kinematic and structural parsing of arthrodire feeding variation (R. K. Carr, personal communication, 2008).

These studies are ultimately important for understanding trophic radiations among gnathostomes. The Gogo Formation was laid down in a reef setting. Reefs today harbor high diversity and disparity of trophic niches (Anderson, 2008). Have reefs consistently been centers of niche variety for 400 Ma, and has the complexity of jaw mechanisms (lower in arthrodires and higher in derived teleosts) governed magnitudes of speciation and divergence? Did negative allometry of jaw stress in *Dunkleosteus* lead to niche partitioning by size more than mechanics? How common and effective are isometric and allometric mandible growth as contributors to functional performance and ecological diversity? With spectacular preservation and simple lower jaws, arthrodires are among the first and best groups for grounding such questions.

References

Anderson, P. S. L. 2008. Shape variation between arthrodire morphotypes indicates possible feeding niches. Journal of Vertebrate Paleontology, 28:961–969.

Anderson, P. S. L. 2009. Biomechanics, functional patterns, and disparity in Late Devonian arthrodires. Paleobiology, 35:312–342.

Anderson, P. S. L. 2010. Using linkage models to explore skull kinematic diversity and functional convergence in arthrodire placoderms. Journal of Morphology, 271:990–1005.

Anderson, P. S. L., and M. W. Westneat. 2007. Feeding mechanics and bite force modeling of the skull of *Dunkleosteus terrelli*, an ancient apex predator. Biology Letters, 3:76–79.

Anderson, P. S. L., and M. W. Westneat. 2009. A biomechanical model of feeding kinematics for *Dunkleosteus terrelli* (Arthrodira, Placodermi). Paleobiology, 35:251–269.

Arbour, V. M., and E. Snively. 2009. Biomechanics and function of the tail club in ankylosaurid dinosaurs. The Anatomical Record, 292:1412–1426.

Bell, P. R., E. Snively, and L. Shychoski. 2009. A comparison of the jaw mechanics in hadrosaurid and ceratopsid dinosaurs using finite element analysis. The Anatomical Record, 292:1338–1351.

Blakey, R. C. 2010. Global Paleogeography. Accessed March 31, 2010. <http://jan.ucc.nau.edu/~rcb7/globaltext2.html>

Carr, R. K. 1991. Reanalysis of *Heintzichthys gouldii* (Newberry), an aspinothoracid arthrodire (Placodermi) from the Famennian of northern Ohio, with a review of brachythoracid systematics. Zoological Journal of the Linnean Society, 103:349–390.

Carr, R. K. 1995. Placoderm diversity and evolution. *In* M. Arsenault, H. Lelievre, and P. Janvier (eds.), Studies on early vertebrates. (VIIth International Symposium, 1991, Miguasha Parc, Quebec.) Bulletin du Museum National d'Histoire Naturelle, Paris, 4e série, C 17(1–4):85–125.

Cook, R. D. 1995. Finite Element Modeling for Stress Analysis. John Wiley & Sons, New York. 320 p.

Currie, P. J. 2003. Allometric growth in tyrannosaurids (Dinosauria: Theropoda) from the Upper Cretaceous of North America. Canadian Journal of Earth Sciences, 40:651–665.

Dingerkus, G., B. Seret, and E. Guilbert. 1991. Multiple prismatic calcium phosphate layers in the jaws of present-day sharks (Chondrichthyes; Selachii). Experientia, 47:38–40.

Dumont, E. R., I. R. Grosse, and G. J. Slater. 2009. Requirements for comparing the performance of finite element models of biological structures. Journal of Theoretical Biology, 256:96–103.

Henderson, D. M., and E. Snively. 2003. *Tyrannosaurus* en pointe: allometry minimized rotational inertia of large carnivorous dinosaurs. Proceedings of the Royal Society B, Biology Letters, 271:S57–S60.

Jaminski, J., T. J. Algeo, J. B. Maynard, and J. C. Hower. 1998. Climatic origin of dm-scale compositional cyclicity in the Cleveland Member of the Ohio Shale (Upper Devonian), Central Appalachian Basin, U.S.A, p. 217–242. *In* J. Schieber, W. Zimmerle, and P. S. Sethi (eds.), Shales and Mudstones. I. E. Schweizerbart'sche Verlagsbuchhandlung, Stuttgart.

Long, J. A., and K. Trinajstik. 2010. The Late Gogo Formation Lägerstatte of Western Australia: exceptional early vertebrate preservation and diversity. Annual Review of Earth and Planetary Sciences, 38:255–279.

Playford, P. E. 1980. Devonian "Great Barrier Reef" of the Canning Basin, Western Australia. American Association of Petroleum Geologists Bulletin, 64:814–840.

Rayfield, E. J. 2004. Cranial mechanics and feeding in *Tyrannosaurus rex*. Proceedings of the Royal Society of London B, 271:1451–1459.

Rayfield, E. J. 2007. Finite element analysis and understanding the biomechanics and evolution of living and fossil organisms. Annual Review of Earth and Planetary Sciences, 35:541–576.

Rieppel, O., and L. Labhardt. 1979. Mandibular mechanics of *Varanus niloticus*. Herpetologica, 35:158–163.

Ross, C. F. 2005. Finite element analysis in vertebrate biomechanics. Anatomical Record, 283:253–258.

Shychoski, L. 2006. A geometric morphometric and finite element analysis investigating tyrannosauroid phylogeny and ontogeny emphasizing the biomechanical implications of scale. Unpublished M.Sc. thesis, University of Bristol, Bristol, England. 125 p.

Shychoski, L., and E. Snively. 2008. Ecological implications of tyrannosaurid lower jaw ontogeny, biomechanical scaling, and bite function. Journal of Vertebrate Paleontology, 28(Supplement to 3):142A.

Slater, G. J., E. R. Dumont, and B. Van Valkenburgh. 2009. Implications of predatory specialization for cranial form and function in canids. Journal of Zoology, 278:181–188.

Snively, E., and A. Cox. 2008. Structural mechanics of pachycephalosaur crania permitted head-butting behavior. Palaeontologia Electronica 11, Issue 1, 3A. 17 p. Accessed March 31, 2010. <http://palaeo-electronica.org/2008_1/140/index.html>

Therrien, F., D. M. Henderson, and C. B. Ruff. 2005. Bite me: biomechanical models of theropod mandibles and implications for feeding behavior, p. 179–237. *In* K. Carpenter (ed.), The Carnivorous Dinosaurs. Indiana University Press, Bloomington.

Tseng, Z. J. 2009. Cranial function in a late Miocene *Dinocrucuta gigantea* (Mammalia: Carnivora) revealed by comparative finite element analysis. Biological Journal of the Linnean Society, 96:51–67.

Tseng, Z. J., and W. J. Binder. 2009. Mandibular biomechanics of *Crocuta crocuta*, *Canis lupus*, and the late Miocene *Dinocrocuta gigantea* (Carnivora, Mammalia). Zoological Journal of the Linnean Society, 158:683–696.

Wroe, S., K. Moreno, P. Clausen, C. McHenry, and D. Cunroe. 2007. High-resolution three dimensional computer simulation of hominid cranial mechanics. Anatomical Record, 290:1248–1255.